

2.1 Spin-Orbit Term in Light Heavy-Ion Elastic Scattering Potential

O. Satoh, T. Yamaya, K. Kotajima†, T. Shinozuka†† and M. Fujioka††

Department of Physics, Tohoku University, Sendai 980, Japan

† Department of Nuclear Engineering, Tohoku University, Sendai 980, Japan

†† Cyclotron and Radioisotope Center, Tohoku University, Sendai 980, Japan

In heavy-ion elastic scattering data at relating low bombarding energies (< 10 MeV per nucleon) which are not very far above the Coulomb barrier, the scattering is sensitive to the potential in the vicinity of the strong absorption radius. For the elastic scattering of spin 1 heavy ion projectiles from spin 0 target nuclei, the total angular momentum of the projectiles is defined by $J = L \pm 1$, where the sign depends on the orientation of the spin of the projectile relative to the orbital angular momentum L . In the general spin-orbit coupling interaction picture, where $V_{LS}(r)$ is negative for $J = L+1$ and positive for $J = L-1$, it is important to note the difference in sign between the parallel and the antiparallel spin-orbit coupling interactions in the region of the strong absorption radius. Projectiles distorted to be nearing the target nuclei by the negative spin-orbit interaction are more strongly absorbed, and on the contrary projectiles distorted to be far from the target nuclei by the positive spin-orbit interaction are more weakly absorbed. The above discussion is qualitatively illustrated in Fig. 1 in the case of ^{14}N elastic scattering on the ^{28}Si target at $E = 84$ MeV. The top of Fig. 1 shows the closest approach distances of projectiles as a function of orbital angular momentum L . The bottom of Fig. 1 shows the reflection coefficients $\eta_L = |\exp(2i\delta_L)|$ as a function of L .

Elastic and inelastic scattering angular distributions of 65 MeV ^{12}C , 75 MeV ^{16}O and 84 MeV ^{14}N ions on the ^{28}Si target have been measured in the angle region of $8^\circ < \theta_{\text{cm}} < 70^\circ$ in step of $\Delta\theta_{\text{cm}} < 1^\circ$. These beams were provided from the Tohoku University 680-cyclotron. The ratios of the experimental differential cross sections to Rutherford scattering are shown in Fig. 2 together with the results of the DWBA calculations. The optical model search code ELAST2¹⁾ was used to fit the elastic scattering data. The two types of potentials by Cramer²⁾ and by Satchler³⁾, called by them the 'deep' which had $V_0 = 100$ MeV and the 'shallow' which had $V_0 = 10$ MeV, have been applied for fitting the present data. Starting from these parameters, the optical potential parameters were adjusted so as to get the best fits to the present data. These parameters are listed in Table I. The optical potential parameters for ^{12}C projectile are in agreement with those for ^{16}O projectile in both of the 'deep' and the 'shallow' type potentials (see Table I). However, the optical model parameters for ^{14}N projectile with spin 1 are markedly different from those for ^{12}C and ^{16}O projectiles. The solid and the dotted curves in Fig. 2 are optical model fits corresponding to the 'deep' and the 'shallow' potentials, respectively, given in Table I. The dashed curve for the $^{14}\text{N}+^{28}\text{Si}$ system in Fig. 2 corresponds to the 'deep' optical potential including the spin-orbit coupling force. In this optical potential, it is noted that the central potential parameters are similar to those for the $^{12}\text{C}+^{28}\text{Si}$ and the $^{16}\text{O}+^{28}\text{Si}$ systems. The inelastic angular distributions for the 2^+ state of ^{28}Si were fitted using also the optical potentials

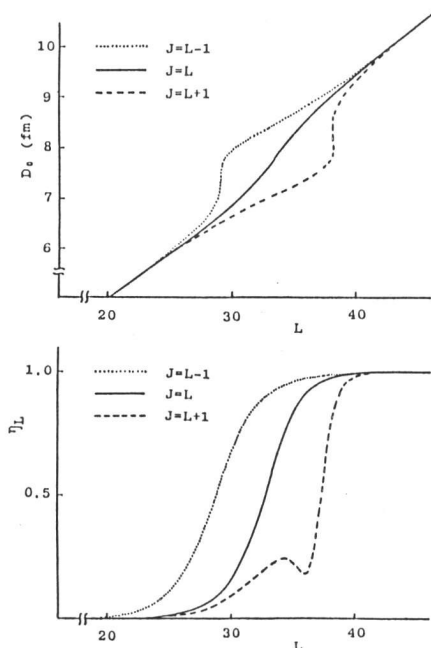


Fig. 1. Location of the closest approach points D_0 (top) and the scattering reflection coefficient η_L (bottom) as a function of the orbital angular momentum L .

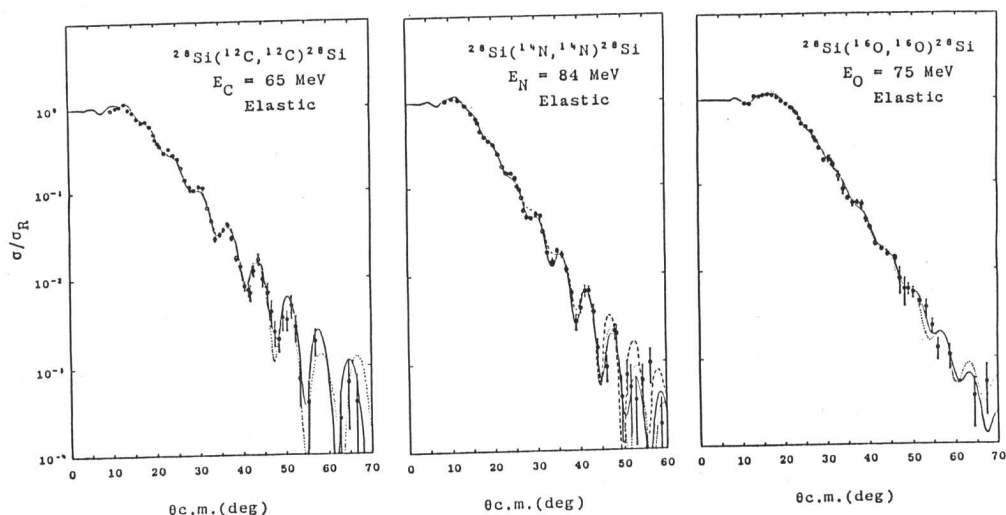


Fig. 2. Angular dependence of the ratio of the cross sections to Rutherford scattering.

listed in Table I. The results of the fits were qualitatively good. Furthermore, coupling to the inelastic channel has been done in the elastic calculations, resulting in a potential which is within several percent equal to the potentials obtained by fitting the elastic angular distributions as given in Table I. On the basis of these results, it is suggested that the spin-orbit coupling force should be considered for the elastic scattering of heavy ions with spin. In the present work, the strength of spin-orbit force of the optical potential at the strong absorption radius was about ten times the spin-orbit coupling force derived, using a single folding method⁴⁾, from the deuteron spin-orbit potential.

Table I. Optical Potential Parameters

	V_0 (MeV)	r_R (fm)	a_R (fm)	W_0 (MeV)	r_I (fm)	a_I (fm)	V_{so} (MeV)	r_{so} (fm)	a_{so} (fm)	r_C (fm)	χ^2/N
$^{12}\text{C}+^{28}\text{Si}$ $E_C = 65$ MeV											
Shallow	10.0	1.397	0.424	21.0	1.279	0.350	—	—	—	1.0	41
Deep	89.8	1.059	0.604	20.7	1.145	0.625	—	—	—	1.3	38
$^{14}\text{N}+^{28}\text{Si}$ $E_N = 84$ MeV											
Shallow	32.6	1.190	0.625	8.62	1.330	0.681	—	—	—	1.0	7.5
Deep	84.8	1.042	0.674	10.1	1.288	0.632	—	—	—	1.2	13
Deep(LS)	89.8	1.059	0.676	20.7	1.171	0.625	0.162	1.778	0.679	1.2	11
$^{16}\text{O}+^{28}\text{Si}$ $E_O = 75$ MeV											
Shallow	10.0	1.397	0.486	21.0	1.296	0.372	—	—	—	1.0	7.1
Deep	89.8	1.059	0.629	20.7	1.176	0.625	—	—	—	1.3	7.2

$$R_i = r_i (A_P^{1/3} + A_T^{1/3})$$

References

- 1) M. Igarashi, Optical model auto search code ELAST2, private communication.
- 2) J.G. Cramer et al., Phys. Rev. C14 (1976) 2158.
- 3) G.R. Satchler, Nucl. Phys. A279 (1977) 493.
- 4) H. Amakawa and K.-I. Kubo, Nucl. Phys. A266 (1976) 521.